High-speed thermoreflectance microscopy using charge-coupled device-based Fourier-domain filtering

Woo June Choi, Seon Young Ryu, Jun Ki Kim, Dong Uk Kim, Geon Hee Kim, and Ki Soo Chang*

Center for Analytical Instrumentation Development, Korea Basic Science Institute (KBSI), 169-148 Gwahak-ro, Yuseong-gu, Daejeon 305-806, South Korea

**Corresponding author: ksc@kbsi.re.kr*

Received June 11, 2013; revised August 14, 2013; accepted August 14, 2013; posted August 16, 2013 (Doc. ID 192110); published September 9, 2013

We present a Fourier-domain filtering method for charge-coupled device (CCD)-based thermoreflectance microscopy to improve the thermal imaging speed while maintaining high thermal sensitivity. The time-varying reflected light distribution from the surface of bias-modulated microresistor was recorded by a CCD camera in free-run mode and converted to the frequency domain using the fast Fourier transform (FFT) for all pixels of the CCD. After frequency peak filtering followed by inverse FFT, a thermoreflectance image was obtained. The imaging results of the proposed method were quantitatively compared with those of the conventional four-bucket method, showing that the Fourier-domain filtering method can provide thermal imaging 24–42 times faster than the four-bucket method, depending on the required thermal sensitivity. © 2013 Optical Society of America

OCIS codes: (110.6820) Thermal imaging; (110.0180) Microscopy; (070.2615) Frequency filtering.
http://dx.doi.org/10.1364/OL.38.003581

Thermoreflectance microscopy (TRM) is a contactless optical imaging technique that provides a two-dimensional (2D) thermal image of microelectronic devices with high spatial and high thermal resolution [1–5]. TRM measures temperature-dependent changes in reflection using the thermo-optic response of a thermally modulated sample. Spatially resolved surface temperature changes (ΔT) of the sample can be obtained from the variation of the optical reflectivity (ΔR) and a linear approximation of the relationship between the temperature change and the reflectivity variation: $\Delta T = \kappa^{-1}(\Delta R/R)$, where R and κ are the optical reflectivity and the thermoreflectance coefficient, respectively [2]. To obtain $\Delta R/R$ with a good signal-to-noise ratio (SNR), various lock-in techniques have been employed in thermoreflectance imaging. A four-bucket method is a prevalent homodyne lock-in technique for charge-coupled device (CCD)-based TRM imaging [2,3]. Since each pixel of the CCD camera effectively performs an independent lock-in measurement at the given thermal excitation frequency, a noise-immune thermal image can be obtained with an improved thermal resolution down to 10 mK under a stochastic resonance regime [3]. However, this method requires averaging over at least three orders of magnitude of iterations (thermal cycles) to achieve the desired thermal sensitivity. This requirement increases the measurement duration time, which can restrict its applicability for fast thermal analysis. Recently, high-speed TRM imaging has been demonstrated using a novel silicon detector chip with a 2D array of pixels [6]. This customized photodiode array incorporated with ac-coupled analog amplifiers and high-precision analog–digital (A/D) converters performed thermoreflectance detection separately at each of the pixels in parallel. This approach allows one to acquire a high-contrast thermal image with improved acquisition speed [6]. However, the complex chip design and smaller number of pixels (16×16 pixels) of the detector may hinder its widespread use in high-resolution thermal imaging applications.

In this Letter, we report a simple and an effective thermoreflectance technique for fast thermal imaging. A Fourier-domain filtering is utilized as an image acquisition strategy for CCD-based TRM, extracting an intrinsic thermoreflectance amplitude from the spectral components of the time-series CCD thermoreflectance signals. This scheme can offer thermal image acquisition in a few seconds with high sensitivity and high spatial resolution. The imaging feasibility of the proposed method is confirmed by quantitative comparison with the conventional four-bucket measurements in thermoreflectance imaging of a biased resistive sample.

The schematic of the optical setup is shown in Fig. 1. A visible light-emitting diode (LED) was used as a probe beam for measuring the reflectivity of the sample. The probe beam evenly illuminated the surface of the sample through a 20-mm-long working distance microscope objective lens (20×, 0.42 N.A.), and the backreflected light field was projected onto a visible CCD camera (1600×1200 pixels, 14 bits) through a bandpass filter

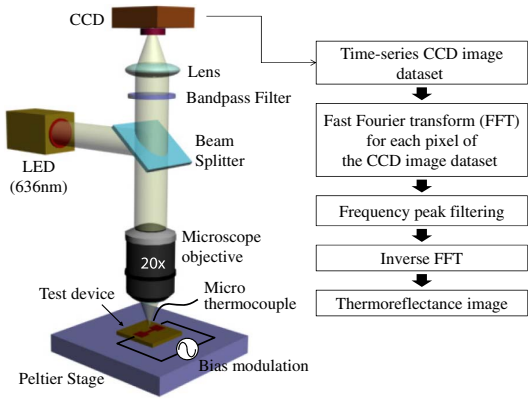

Fig. 1. Schematic of the CCD-based TRM setup.

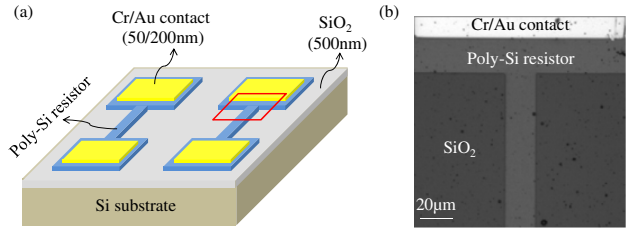

Fig. 2. (a) Schematic of a polycrystalline silicon (poly-Si) resistor sample. (b) Microscope image of the resistor [at the position indicated by the red box in (a)].

centered at the wavelength of the probe beam. A stripe-patterned polycrystalline silicon (poly-Si) resistor (0.3 μm thick, 20 μm wide, and 200 μm long) deposited on a SiO_2(500 nm)/Si substrate with Cr/Au ohmic contacts was used as a planar resistive sample [$R = 350\ \Omega$; Fig. 2(a)]. To maximize the thermal sensitivity, we selected a red LED with a center wavelength of 636 nm as a probe beam, which elicited a strong thermoreflectance response from the surface of the poly-Si resistor. The imaged area of the resistor sample (160 μm × 160 μm) is shown in Fig. 2(b), corresponding to 200 × 200 CCD pixels. The temperature of the microresistor substrate was stably maintained at 25 ± 0.005°C using an active feedback loop with a Peltier stage and a microthermocouple on the substrate.

When the poly-Si resistor was powered with a 1 Hz sine wave (5.0 V peak-to-peak, 2.5 V DC offset), temperature-induced reflectance modulation was exhibited on the surface of the resistor. Thus, the time-varying reflected probe signals were successively detected with the 50 Hz CCD camera in free-run mode (that is, not phase-locked with the thermal modulation of the sample) and stored. From the stored multiple CCD frames containing time-series thermoreflectance data, the reflected intensity signal at an arbitrary pixel location in the resistor area was taken, as shown in Fig. 3(a), and converted to the frequency domain using the fast Fourier transform (FFT), yielding spectral peaks containing the bias modulation frequency of 1 Hz and high-order harmonics due to Joule heating for the region of the resistor [Fig. 3(b)]. The first harmonic (1 Hz) of the FFT spectrum was decoupled from the noise and the high-order harmonics with filtering based on frequency of the peak and was then converted into the time domain using an inverse FFT. The broader filtering window will include spurious frequency components, which can induce amplitude fluctuation in the modulation cycles, leading to an error of modulation amplitude (ΔR) value. The modulation amplitude (ΔR) was calculated by averaging the temporal amplitudes

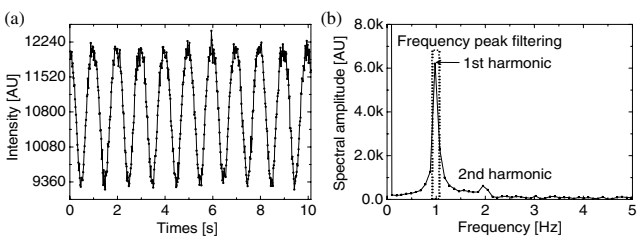

Fig. 3. (a) Temporal profile taken at an arbitrary pixel point in the resistor area and (b) its FFT spectrum.

of the thermoreflectance modulation cycles. As such a modulation amplitude was obtained for each of the pixels of the CCD, a ΔR image was achieved and normalized with the initial background reflectivity (R), giving a thermoreflectance image ($\Delta R/R$).

The conventional four-bucket method was also performed with the same TRM microscope and the same sample under identical bias conditions (1 Hz sine wave, 5 V peak-to-peak, 2.5 V DC offset). However, the CCD frame rate should be set to 4 Hz because the bias modulation (1 Hz) was phase-locked to the CCD frame triggered at four times the bias modulation frequency. The thermoreflectance signals were integrated with the CCD camera during the four quarters of the bias modulation period, and thus, four CCD frames were recorded during each period of the thermal modulation. A thermoreflectance image ($\Delta R/R$) was then obtained by a simple calculation from these four frames [2]. Cumulative averaging over the TRM measurement results could be used to improve the thermal sensitivity.

Figure 4(a) shows a thermoreflectance image of the biased poly-Si resistor obtained with 500 CCD frames using the Fourier-domain filtering method. In Fig. 4(a), a T-shaped thermoreflectance signal is clearly visible in the image, which corresponds to the poly-Si resistor region of Fig. 2(b). The spatial resolution of the thermoreflectance image was experimentally measured to be 845 nm by taking the derivative of the profile taken across the side of the poly-Si resistor [the solid line in Fig. 4(a)] [7]; this gives a good approximation to the 712 nm resolution theoretically achievable using the Sparrow criterion under the same illumination wavelength (636 nm) and microscope objective lens N.A. value (0.42). The background noise in the thermoreflectance was calculated from the standard deviation of the thermoreflectance image ($\Delta R/R$) [3]. Using 175 [5 (X) × 35 (Y)] adjacent pixels in an area that appeared relatively uniform and to have constant-amplitude intensity variation on the surface of the poly-Si resistor during temperature modulation [indicated by the dotted box in Fig. 4(a)], we were able to determine the standard deviation to be 3.6×10^{-4}, representing the thermal sensitivity. Figure 4(b) shows the evolution of the thermal sensitivity and the measurement duration time (CCD frame acquisition time + evaluation time) as a function of the number of measurement iterations (N), respectively. One iteration includes 50 CCD frames. In this figure, as N increases, a progressively smaller

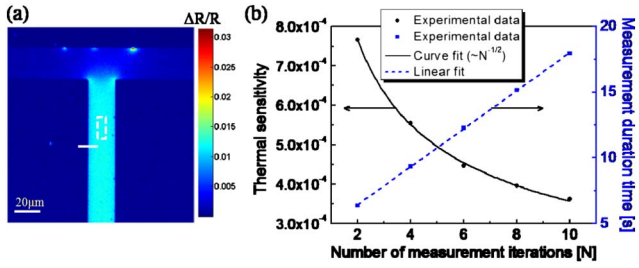

Fig. 4. (a) Thermoreflectance image of the poly-Si resistor sample. (b) Evolution of the thermal sensitivity and the measurement duration time as a function of the number of measurement iterations (N).

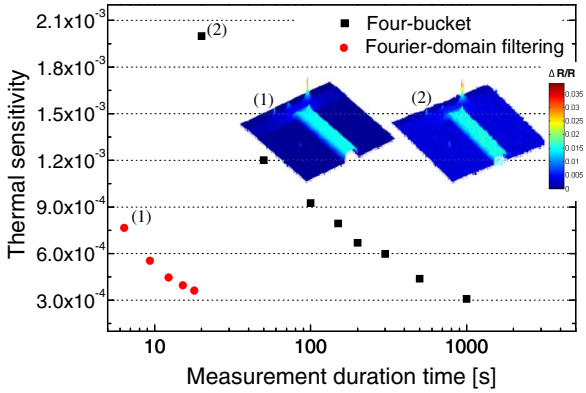

Fig. 5. Thermoreflectance sensitivity measurements against the measurement duration time using the Fourier-domain filtering method and the four-bucket method. The insets in the figure are surface plots of the thermoreflectance images corresponding to measurements (1) and (2), respectively.

thermoreflectance signal is detectable. It is noted that the fit curve to the thermal sensitivity data was inversely proportional to the square root of the number of accumulated CCD frames ($N \times 50$). This nonlinear trend is also found in thermal sensitivity measurements of the conventional lock-in thermography and the CCD-based TRM method [3,8]. However, the measurement duration time is linear with the number of accumulated CCD frames, ranging from 6.4 to 17.9 s for 100–500 CCD frames in our experiment.

To evaluate the thermal imaging performance of the proposed method, the thermal sensitivity values were compared with results using the four-bucket method, calculated with the same region of interest in thermoreflectance images taken with different numbers of iterations: 20, 50, 100, 150, 200, 300, 500, and 1000. The resulting two thermal sensitivity datasets are each plotted against the measurement duration time in Fig. 5. In Fig. 5, we can see that all of the thermoreflectance sensitivity values of the Fourier-domain filtering method are obtained in 20 s, below those of the four-bucket method obtained in 150 s or less. This means that the Fourier-domain filtering method is able to detect a small signal in a shorter measurement time than the four-bucket method. This can be clearly seen from the two thermoreflectance images of the microresistor (in the insets in Fig. 5) obtained with the Fourier-domain filtering (1) and four-bucket (2) methods, respectively, in Fig. 5, where thermoreflectance image (2) appears to be somewhat noisier than (1).

The measurement duration time cost to achieve the same thermal sensitivity value with each of the methods was quantitatively compared. The four-bucket detection data was curve-fitted to find the expected measurement duration times for the thermal sensitivity values equal to the five Fourier-domain filtering data points. The results are summarized in Table 1, showing that the Fourier-domain filtering method achieves the same thermal sensitivity 24–42 times faster than the four-bucket method. In our view, this difference may be due to the limited CCD frame acquisition rate of the four-bucket measurement. That is, the CCD camera in the four-bucket detection must be phase-locked with the bias modulation of the sample and triggered at four times the modulation

Table 1. Measurement Duration Time Required to Achieve the Same Thermal Sensitivity Value

	Measurement Duration Time (s)	
Thermal Sensitivity/ [a]Thermal Resolution (mK)	Fourier-Domain Filtering Method	Four-Bucket Method
7.66×10^{-4}/330	6.4	154.1
5.54×10^{-4}/230	9.3	260.8
4.46×10^{-4}/192	12.3	476.5
3.95×10^{-4}/170	15.2	639.0
3.60×10^{-4}/155	17.9	762.1

[a]Thermal resolution is obtained using a thermoreflectance coefficient $\kappa = -2.32 \times 10^{-3}$ K^{-1} measured using the method described in [7].

frequency of 1 Hz, whereas the Fourier-domain approach is free from such a limit, allowing the maximal frame rate (50 Hz in our experiment) of the CCD camera to be used, which enables the accumulation of more CCD frames over a given time. Considering the inverse proportionality between the square root of the number of accumulated CCD frames and the thermal sensitivity, the Fourier-domain filtering method should reach the required thermal sensitivity much sooner than the four-bucket method. These experimental findings confirm that the proposed method is able to guarantee fast thermal imaging compared to the conventional TRM measurement. At higher thermal modulation frequencies and a higher CCD frame rate, we expect that the measurement duration time can be shorter for both methods. However, there should be some upper limit on the thermal modulation frequency because it is limited by the thermal response time of the sample, the maximum CCD frame rate, and the low SNR of the CCD with a short integration time. Future study regarding this will be worthwhile to further improve the thermal imaging speed. In Table 1, the measured thermal resolution is significantly larger than the theoretical value corresponding to the quantization bin size of the CCD camera ($\kappa^{-1}/2^b = 26$ mK, where b is the bit depth of the CCD camera) [2]. From the experimental standpoint, there are several possible noise sources whose noise level is larger than the quantization bin size that might reduce the thermal resolution beyond the nominal value, namely, an unstable optical output power from the probe beam, and the mechanical instability of the system changing the amount of collected light during measurement. Also of concern for the thermal resolution measurement is the rough surface of the sample increasing the standard deviation (noise) of the measured thermoreflectance signal. Further quantitative study regarding these issues is currently underway.

In summary, we have demonstrated the use of a Fourier-domain filtering method in high-resolution CCD-based thermoreflectance imaging and compared the results with those of the conventional four-bucket method. The experimental results showed that the Fourier-domain filtering method could offer high-sensitivity thermoreflectance imaging at a faster imaging speed than the conventional four-bucket method. Moreover, the Fourier-domain filtering provides a simple implementation of thermal imaging because of its freedom

from the need for phase locking between the CCD camera and the thermal modulation of the sample. These advantages suggest that this new TRM approach will become a promising alternative for applications where rapid thermal inspection is needed, such as for failure analysis in semiconductor device production lines.

This work was partially supported by a KBSI grant (D33200) and an SMBA grant (S2060032).

References

1. G. Tessier, S. Holé, and D. Fournier, Appl. Phys. Lett. **78**, 2267 (2001).
2. M. Farzaneh, K. Maize, D. Lüerβen, J. A. Summers, P. M. Mayer, P. E. Raad, K. P. Pipe, A. Shakouri, R. J. Ram, and J. A. Hudgings, J. Phys. D **42**, 143001 (2009).
3. P. M. Mayer, D. Lüerβen, R. J. Ram, and J. Hudgings, J. Opt. Soc. Am. A **24**, 1156 (2007).
4. P. E. Raad, P. L. Komarov, and M. G. Burzo, Microelectron. J. **39**, 1008 (2008).
5. J. Kim, S. Han, T. Walsh, K. Park, B. J. Lee, W. P. King, and J. Lee, Rev. Sci. Instrum. **84**, 034903 (2013).
6. J. Christofferson and A. Shakouri, Rev. Sci. Instrum. **76**, 24903 (2005).
7. G. Tessier, M.-L. Polignano, S. Pavageau, C. Filloy, D. Fournier, F. Cerutti, and I. Mica, J. Phys. D **39**, 4159 (2006).
8. O. Breitenstein and M. Langenkamp, *Lock-in Thermography—Basics and Use for Functional Diagnostics of Electronic Components* (Springer, 2003).